Wave period retrieval from altimeters

Y. Quilfen (1), B. Chapron (1), F. Collard (2), M. Serre (3)
(1) Ifremer, (2) Boost Technologies, (3) University of North Carolina

__Abstract__: The altimeter radar backscatter cross-section (NRCS) is known to be related to the ocean surface wave slope statistics, linked to the surface acceleration statistics according to the surface wave dispersion relationship. Since altimeter measurements also provide significant wave height (SWH) estimates, we propose to derive empirical altimeter wave period models by combining both NRCS and SWH measurements with the neural network methodology. It is shown that using dual-frequency measurements improves mean wave period retrieval. Altimeter mean wave period estimates are compared with the NDBC buoy data and with the WaveWatch-III numerical wave model to illustrate their usefulness for wave models tuning and validation (accepted in Marine Geodesy, 2004).

I - Neural network architecture and training process

The main advantage of using neural networks to define an altimeter mean wave period (Tm) model is that it does not require an a priori knowledge of the relation linking the different variables. The neural model is calibrated upon a set of Topex/Poseidon (T/P) altimeter measurements co-located with the National Data Buoy Center (NDBC) buoys. The NDBC data have been collected over the period spanning from October 1992 to March 2002 by 33 buoys. Two models have been defined, the first using only Ku-band NRCS and SWH as inputs (NN-1), the second using in addition C-band NRCS and wind speed to better account for the sea state maturity (NN-2). These models are compared with a former one developed at Southampton Oceanographic Center (SOC).

$$tnn_1 = e^{-17.1642 \times a + 13.5844} \quad ; \quad a = \frac{1}{1 + e^{0.6573 \times Hs^{0.1084} \times \sigma_{Ku}^{0.2942} - 2.2377}}$$

$$tnn_2 = e^{5.7474 - 1.4688 \times a + 1.7943 \times b} \quad ; \quad a = \frac{\sigma_{Ku}^{0.3082}}{\sigma_c^{0.2352} \times Hs^{0.0981}} \times e^{1.5068 \times b}$$

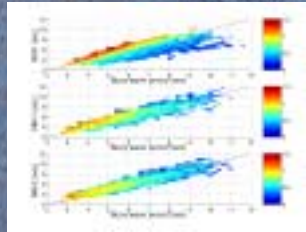$$b = \frac{2}{1 + e^{-1.8612 - 0.08 \times U_{10}}} - 1$$

Figure 1: Comparisons of altimeter wave period models with the NDBC buoy wave period, color-coded as a function of the inverse wave age

model	SOC			NN-1			NN-2		
Correlation	0.78	0.59	0.78	0.88	0.83	0.82	0.91	0.87	0.82
Bias (model – buoy, sec)	-0.5	-0.28	-0.2	0.03	0.23	0.08	-0.02	0.16	0.06
Std deviation (sec)	1.05	0.9	0.64	0.81	0.63	0.53	0.7	0.54	0.51

Table 1: Comparison between the buoy wave period and the altimeter SOC, NN-1 and NN-2 models, for the global data-set (left, 5904 points), the Hawai area (midde, 693 points), and the Gulf of Mexico area (right, 1370 points).
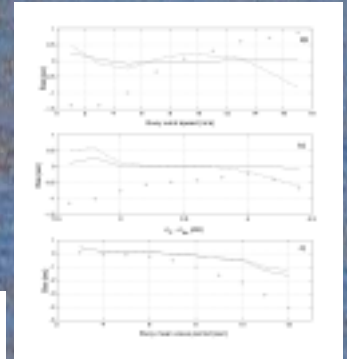

Figure 2: Mean wave period bias (altimeter minus buoy) as a function of: a) the buoy wind speed; b) the difference in the C and Ku bands NRCS; c) the buoy mean wave period. NN-2 (solid line), NN-1 (dashed line), and SOC (crosses).
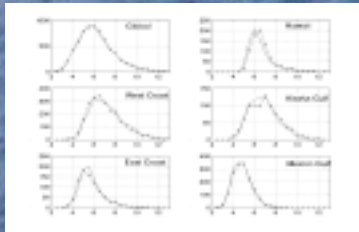

Figure 3: Distribution of buoy (solid line) and altimeter (dashed line) wave period measurements (sec) for the different areas covered by NDBC buoys.

II - Local climatology

On Figure 3 are displayed histograms of the buoy and T/P altimeter NN-2 wave period measurements for the global data set and for the specific areas covered by the NDBC buoy network. The histogram features (maximum, shape and tail) are nicely reproduced with the NN-2 model. The histograms are relatively spreaded in the West Coast and Alaska Gulf regions, featuring variable local conditions and frequent mean wave periods greater than 10 s. These large mean wave periods correspond to high wind seas and long swells propagating across the Pacific ocean. At the opposite, the Mexico Gulf histogram is sharper with a lower peak value and very few mean wave periods greater than 8 s are encountered because long swells are unable to develop. In the Hawai region, the histogram is also sharp because of the steady trade winds and the peak value of 6 s corresponds to mixed wind seas and swell trains.

III - Comparison with WaveWatch-III numerical model

Figure 4, right panels, compares the T/P and NDBC Tm as a function of the T/P wind (January months, 1992-2002) for further validation. The left panels showing the comparison with WW3 thus indicates underestimation of the WW3 Tm over the whole wind speed range, at the exception of the Mexico Gulf. The long swells cannot developed in this region and the wave climate is thus dominated by the wind seas. This feature and the systematic WW3 mean wave period underestimation at low wind speed may indicate that the numerical model underestimates systematically the swell part of the wave spectrum in the used configuration. On the other hand, there is an excellent agreement between the WW3 and T/P significant wave heights, suggesting that the wind forcing is adequate (merged QSCAT scatterometer and NCEP winds). Underestimation of the WW3 Tm may be attributed to the wave model physics or parameterizations. The altimeter Tm can thus be used as an interesting additional parameter for numerical model tuning and physics understanding.
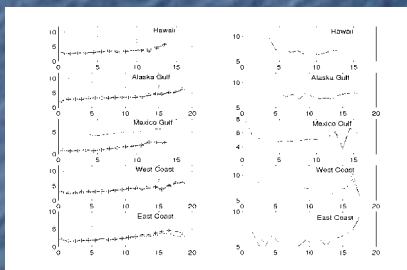

Figure 4: T/P (solid line, all panels), NDBC buoy (dashed line, right panel), and WW3 (dashed line, left panel) Tm as function of T/P wind. Mean wave heights (m) are displayed on left panel for T/P (plus) and WW3 (circles). The measurements cover January 2003 (left panel) and the January months for the time period 1992-2002 (right panel).

IV – T/P and JASON-1 cross-calibration

The neural models have been calibrated for T/P measurements but can also be used to estimate Tm with Jason data taking into account the differences in NRCS calibration. Mean Tm fields can thus been derived for Jason and compared with the T/P ones for the January month (Figure 5). Excellent agreement is obtained and a merged product has been derived.
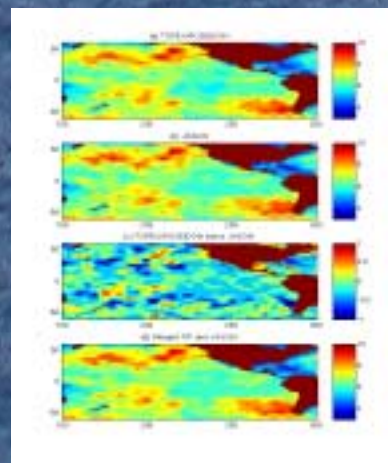

Figure 5: Mean altimeter wave period fields computed with T/P (a), JASON (b), the mean difference (c), and the field from merged T/P and Jason data (d), January 2003. All units are in seconds.